Biogeosciences, 20, 619–633, 2023
https://doi.org/10.5194/bg-20-619-2023

Biogeosciences
Open Access
EGU

Seasonal variation of mercury concentration of ancient olive groves of Lebanon

Nagham Tabaja[1,2,3], David Amouroux[4], Lamis Chalak[2], François Fourel[5], Emmanuel Tessier[4], Ihab Jomaa[6], Milad El Riachy[7], and Ilham Bentaleb[1]

[1]University of Montpellier, UMR 5554 CNRS/IRD/EPHE, CC061 Montpellier, France
[2]Faculty of Agronomy, Plant Production Department, The Lebanese University, Dekwaneh, Lebanon
[3]Plateforme de Recherche et d'Analyses en Sciences de l'Environnement (PRASE), Ecole Doctorale de Sciences et Technologie, Université Libanaise, Hadath, Lebanon
[4]Institut des Sciences Analytiques et de Physico-Chimie pour l'Environnement et les Matériaux (IPREM), Université de Pau et des Pays de l'Adour, E2S/UPPA, CNRS, PAU, France
[5]UMR CNRS 5023 LEHNA, Université Claude Bernard Lyon 1, Villeubanne, France
[6]Department of Irrigation and Agrometeorology, Lebanese Agricultural Research Institute (LARI), P.O. Box 287, Zahle, Lebanon
[7]Department of Olive and Olive Oil, Lebanese Agricultural Research Institute (LARI), P.O. Box 287, Zahle, Lebanon

Correspondence: Ilham Bentaleb (ilham.bentaleb@umontpellier.fr)

Received: 8 April 2022 – Discussion started: 19 July 2022
Revised: 27 December 2022 – Accepted: 5 January 2023 – Published: 6 February 2023

Abstract. This study investigates the seasonality of the mercury (Hg) concentration of olive tree foliage, an iconic tree of the Mediterranean basin. Hg concentrations of foliage, stems, soil surface, and litter were analyzed on a monthly basis in ancient olive trees growing in two groves in Lebanon, Bchaaleh and Kawkaba (1300 and 672 m a.s.l. respectively). A significantly lower concentration was registered in stems ($\sim$ 7–9 ng g^{-1}) in comparison to foliage ($\sim$ 35–48 ng g^{-1}) in both sites, with the highest foliage Hg concentration in late winter–early spring and the lowest in summer. It is noteworthy that olive fruits also have low Hg concentrations ($\sim$ 7–11 ng g^{-1}). The soil has the highest Hg content ($\sim$ 62–129 ng g^{-1}) likely inherited through the cumulated litter biomass ($\sim$ 63–76 ng g^{-1}). A good covariation observed between our foliage Hg time series analysis and those of atmospheric Hg concentrations available for southern Italy in the western Mediterranean basin confirms that mercury pollution can be studied through olive trees. Spring sampling is recommended if the objective is to assess the trees' susceptibility to Hg uptake. Our study draws an adequate baseline for the eastern Mediterranean and the region with similar climatic inventories on Hg vegetation uptake, in addition to being a baseline to new studies on olive trees in the Mediterranean to reconstruct regional Hg pollution concentrations in the past and present.

1 Introduction

Mercury (Hg) is among the most widely distributed, potentially toxic metals polluting the Earth (Briffa et al., 2020). It is founded, as with all heavy metals, naturally on the Earth's crust reservoir and in the atmosphere through the natural long-term Hg biogeochemical cycle (i.e., volcanic activities, geological weathering). This metal is easily modified into several oxidation states, and it can also be spread through many ecosystems (Boening, 2000). The natural Hg cycle has been modified due to anthropogenic activities (i.e., mining, smelting, soil erosion due to deforestation, gold extraction, agriculture fertilizers, manure; Patra and Sharma, 2000). Among natural and anthropogenic Hg emissions, inorganic elemental Hg (Hg(0)) is the most dominant chemical form. It is primarily transferred through the atmosphere by air mass movement and can undergo long-range transport. Because of its high volatility and susceptibility to oxidation, elemental Hg(0) is the predominant form of Hg in the atmo-

sphere that can be accumulated into foliage. This highly diffusive Hg can easily pass biological barriers (i.e., cell membranes, foliage, skin). Mercury has three oxidation states, namely, Hg(0) (elemental mercury), Hg(I) (mercurous), or Hg(II) (mercuric), although the Hg(I) mercurous form is not stable under typical environmental conditions and, therefore, is rarely observed. It is likely that the Hg(II) high binding affinities bind covalently with organic groups (Du and Fang, 1983; Clarkson and Magos, 2006; Pleijel et al., 2021). The exchange of Hg between the soil and plants is not stable and is variable dependent (e.g., cation-exchange capacity, soil pH, soil aeration, and plant species; Patra and Sharma, 2000). Forests are known to act as a sink of atmospheric Hg (Hg_{atm}). Plant foliage takes up Hg deposited on leaf surfaces through the stomata (i.e., leaf gas exchange) and leaf cuticles (Hanson et al., 1995; Jiskra et al., 2018; Li et al., 2017b; Lodenius et al., 2003; Maillard et al., 2016; Rea et al., 2002; Yanai et al., 2020), where it accumulates with minimal mobility and where small portions are released back into the atmosphere or transferred to other plant organs (Cavallini et al., 1999; Hanson et al., 1995; Li et al., 2017a; Lodenius et al., 2003; Schwesig and Krebs, 2003). All together, these authors contributed to highlighting the dynamic role of the foliar surfaces in terrestrial forest landscapes acting as a source or sink dependent on the magnitude of current Hg concentrations. Hanson et al. (1995) suggested species-specific compensation concentrations (or compensation points) for Hg deposition.

Hg is redistributed to the forest floor through litter and throughfall and hence passes to the soil (Rea et al., 1996). The Hg input through the litter is greater than the input from that of the wet deposition (Wang et al., 2016). Litter has been estimated to constitute 30 % to 60 % of the Hg atmospheric deposition in European and North American forests (Rea et al., 1996; Blackwell and Driscoll, 2015; Zhou et al., 2018). According to Wright et al. (2016), the litter Hg is the dominant pathway in forests, where it contributes 53 % to 90 % of the dry deposition to the forest. In terrestrial ecosystems, soils have the highest Hg reservoir (Obrist et al., 2018; O'Connor et al., 2019) followed by trees (Yang et al., 2018). This Hg is provided by natural geological sources, natural events such as forest fires and volcanic eruptions (Ermolin et al., 2018; Obrist et al., 2018; O'Connor et al., 2019), and anthropogenic sources (UNEP, 2019). Though variable from year to year, Hg emission to the atmosphere from biomass burning is considered as an important driver of the global Hg biogeochemical cycle (Friedli et al., 2009; McLagan et al., 2021; Dastoor et al., 2022). Soil can also release Hg to the atmosphere (Luo et al., 2016; Assad, 2017; Yang et al., 2018; Schneider et al., 2019; Gworek et al., 2020; Pleijel et al., 2021) and also behave as a source of Hg to the plants. Hg of the soil is taken up by the roots along with the water, following which it is translocated to other parts (i.e., stems, leaves) of the plant using the xylem sap (Bishop et al., 1998; Li et al., 2017). This pathway has been described in several plant species in Hg-contaminated sites (Assad et al., 2017). Trees are hence considered as important drivers of Hg exchange between the atmosphere and the soil (Yang et al., 2018). The recent studies on Hg uptake by vegetation have highlighted the importance of the role of different parameters such as vapor pressure deficit, soil water content, climatic conditions, date of sampling, leaf mass area, tree functional groups, and stomatal conductance, potentially affecting the root uptake of Hg dissolved in soil water, the absorption rate via stomata, and eventually, the Hg leaf content (Rea et al., 2002; Obrist et al., 2011; Blackwell and Driscoll, 2015; Yang et al., 2018; Wohlgemuth et al., 2021). In polluted sites, the soil is the main source of Hg to the vegetation, while away from those sites, the atmosphere is the most important source (Naharro et al., 2018). The Hg source in foliage varies with respect to the amount of contamination (Hanson et al., 1995).

The studies of the Hg cycle in forest ecosystems show that gaseous elemental Hg(0) is the main source taken up by plants (Bishop et al., 2020; Zhou et al., 2021). Analysis of long-term $Hg(0)_{atm}$ and CO_2 concentrations are very informative for understanding the role of vegetation in the global Hg cycle (Jiskra et al., 2018). Emission reduction measures adopted in Europe and North America since the 1970s are corroborated by Hg dendrochemistry analysis, which shows a declining Hg concentration trend from the older to newer tree rings. Indeed, tree ring Hg (dendrochronology) is a powerful archiving tool for $Hg(0)_{atm}$. After Hg(0) oxidation inside the leaves, Hg(II) binds to organic compounds and then is transported to the bole wood via the phloem (Beauford et al., 1977; Lindberg et al., 1979). This is corroborated by the recent study of McLagan et al. (2022) that shows the benefit of the stable Hg isotope analysis to dendrochemistry. Several studies have evidenced seasonal variations of the $Hg(0)_{atm}$ contents (i.e., in the temperate Northern Hemisphere by Jiskra et al., 2018; in the western Mediterranean Basin in southern Italy; Martino et al., 2022), with high values in winter and low values in summer. Interestingly, Jiskra et al. (2018) also show a significant positive correlation between the monthly Hg(0) and CO_2 concentrations. They highlighted a 1-month offset in Hg(0) summertime minima in September in comparison to the CO_2 minima value occurring in August. This trend is not observed in wintertime. The uptake of Hg(0) by the vegetation continues during CO_2 respiration periods during the fall and night, when the ecosystem exchange of CO_2 turns from being a sink to becoming a source (Wofsy et al., 1993; Jiskra et al., 2018).

The total gaseous Hg (TGM) in the Mediterranean atmosphere is similar to that in northern Europe (1.3 to 2.4 ng m^{-3}) (Kotnik et al., 2014). In the case of a semi-closed sea such as the Mediterranean basin with warm summers, high seawater evaporation, solar radiations, and Hg anthropogenic sources, the Mediterranean Sea acts as a net source of Hg to the global atmosphere (Kotnik et al., 2014), making the Mediterranean an air pollution emission area (Baayoun et al., 2019; Borjac et al., 2019).

The olive tree (*Olea europaea L.*) is one of the most distinctive Mediterranean agro-ecosystem tree species (Besnard et al., 2013) and has adapted to drought (Sghaier et al., 2019). Considered to be among the oldest trees in the Mediterranean basin, centennial olive trees are still growing in many countries along both the eastern and western shore, surviving numerous stresses, and are of considerable historical, cultural, and ecological importance (Terral et al., 2004). The olive tree still remains a key component of agriculture today and will be into the future. Therefore, genetic characterization of olive varieties and genetic resources (Khadari et al., 2019; Galatali et al., 2021), description based on the morphological characteristics and phenology of the growth stages of olive trees (Sanz-Cortés et al., 2002), and experimentation through field irrigation and/or, more rarely, through drought stress treatments (Alcaras et al., 2016) have been conducted to avoid genetic erosion, to optimize the water use for irrigation and hence to improve orchard management, and solely to better understand the biodiversity. Only a few studies have focused on the response of the olive tree to Hg pollution in its natural Mediterranean environment (Higueras et al., 2012, 2016; Guarino et al., 2021; Labdaoui et al., 2021).

Lebanon, a small country in the eastern Mediterranean, is facing important anthropogenic pressure within a changing environment (Gérard and Nehmé, 2020). The air quality all over the country in Lebanon is noted to be moderately unsafe, with an annual mean concentration of $31\,\mu g\,m^{-3}$ of $PM_{2.5}$ (particulate matter), which is above the maximum recommended value ($10\,\mu g\,m^{-3}$; Lebanon: Air Pollution IAMAT 2020). Adding to that, soil samples collected from different areas in southern Lebanon showed values of Hg concentration ranging between 160–6480 $ng\,g^{-1}$, showing high contamination levels (Borjac et al., 2020), as indicated by the World Reference Base for Soil Resources (Senesil et al., 1999; Kabata-Pendias and Pendias, 2000). The main contributors to the air pollution include cement industries, mineral and chemical factories, vehicles emissions, food processing, and oil refining. Ancient olive groves are found across different agro-climatic areas at different altitudinal belts, still producing olives and oil for consumption with these various pollution pressures.

In this study two sites, known for their century-old olive groves and located at two different altitudes in Lebanon, were selected to assess their Hg contents. In these remote areas, no direct sources of mercury contamination are reported, and hence, we expect very low Hg concentrations. However, due to atmospheric transport of Hg, dry or wet deposition of Hg can be expected in remote areas (Grigal, 2003). The main objectives of this study are to examine and compare Hg levels measured in the foliage, stems, fruits, litter, and soil in each of these two olive groves, which we monitored monthly for 18 months. The second objective is to analyze the relative importance of Hg uptake by the soil and foliage in comparison with the Hg_{atm}. Since the distribution of Hg pollution is by nature geographically widespread and given the extent of Hg pollution in the Mediterranean and the transfer of pollution by wind and the Mediterranean Sea, long-distance contamination occurs over large areas. This study may draw an adequate baseline for the eastern Mediterranean and for regions of similar climates inventories in terms of Hg vegetation uptake and for new studies on olive trees in the Mediterranean to reconstruct regional Hg pollution concentrations in the past and present.

2 Materials and methods

Two monumental olive groves were chosen in the context of their historical and agricultural importance, since these two sites are considered to contain olive trees of more than 1400 years old and that are still productive.

2.1 Geographic setting and environmental context

2.1.1 Bchaaleh site – North Lebanon

This grove is situated in the Batroun District (latitude 34°12′06″ N, longitude 35°49′23″ E, altitude 1300 m a.s.l.; Fig. 1). Olive trees are growing, rainfed, in a sandy-loam-textured soil of grain size; sand, silt, and clay percentages are 52.8 %, 38.7 %, and 10.7 % respectively. The soil pH is 7.07 ± 0.26, and the organic matter and calcium carbonate contents are 1.7 % and 38.3 % respectively (Yazbeck et al., 2018). In this study, soil profiles of carbon and nitrogen contents were analyzed. Organic carbon contents decreased with soil depth from about 4 % at 0–1 cm (soil surface) to 2.7 % at 30–60 cm. The total nitrogen is about 0.3 % at 1 cm depth and 0.2 % at 30–60 cm depth. The olive trees are located on two terraces. The first terrace is at 1.5 m above the road level, while the second is at the road level. They have been maintained by the municipality for the last four decades as an endowment property. Precipitation average ranges between 229 and 392 mm in winter and between 0 and less than 2 mm per season in summer, while average temperature is between 4 and 8 °C in winter and between 20 and 23 °C in summer, with an average relative humidity of 63 % (data extracted from LARI (Lebanese Agricultural Research Institute) climatic data; Table S1, Fig. S1 in the Supplement).

The village is at about 36 km from Chekka town, which is located at a lower altitude (0–200 m a.s.l.) nearby the sea (Fig. 1) and is classified as a source of air pollution (EJOLT, 2017). Chekka is the site of an important national cement factory responsible for carbon dioxide, sulfur dioxide, nitrous oxides, carbon monoxide, and particulate material emissions that cause respiratory and health issues (Kobrossi et al., 2002) and for water pollution (Nassif et al., 2016). At 28 km from Bchaaleh, the small commercial port of Selaata (0–37 m a.s.l.) emits many pollutants (i.e., phosphogypsum, heavy metals, radionuclides), expanding via water and air pathways (Petrlik et al., 2013; Yammine et al., 2010). To our knowledge, no direct Hg pollution is reported at the

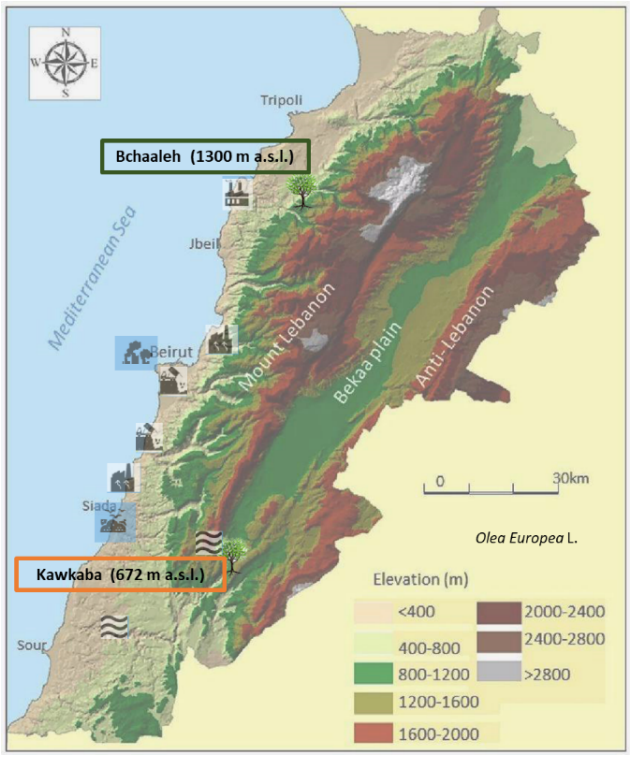

Figure 1. Site locations of the two selected focus areas (modified after Shared Water Resources of Lebanon, Nova Science Publishers, 2017).

Chekka and Selaata sites. However, a dissolved gaseous Hg from natural and human activities is saturated in the upper eastern Mediterranean Sea. Gårdfeldt et al. (2003) have evidenced that the Mediterranean Sea is a source of airborne elemental Hg.

2.1.2 Kawkaba site – South Lebanon

The second grove is located in the village of Kawkaba, South Lebanon (latitude 33°23′856″ N, longitude 35°38′588″ E, altitude 672 m a.s.l.; Fig. 1). Kawkaba soil is characterized as clay loam soil of pH 7.5 ± 0.5. Soil organic material and calcium carbonate averages are 1.7 % and 59.0 % respectively (Al-Zubaidi et al., 2008), and grain size analysis of sand, silt, and clay percentages are 6 %, 28 %, and 66 % respectively. The analysis of organic carbon and nitrogen at 0–1 cm and at 0–30 cm indicates a decrease from about 9.0 % to 2.2 % and from 0.9 % to 0.3 % for carbon and nitrogen respectively. Average precipitation ranges between 215 and 374 mm in winter and drops to almost zero mm in summer, while average temperature is between 7 and 11 °C in winter and between 21 and 27 °C in summer, with relative humidity of 61 % (data extracted from LARI climatic data; Table S1, Figure S1).

The village has to its east the Hasbani river, originating from the northwestern slopes of Mount Hermon in Hasbaya (36 km away from Kawkaba and located at 750 m a.s.l.; Badr et al., 2014; Jurdi et al., 2002). On the other hand, the Litani River (170 km long and located at 800 to 1000 m a.s.l.; Fig. 1) rising in the south of the Bekaa valley is about 29 km away from Kawkaba (Abou Habib et al., 2015; Khatib et al., 2018). These two rivers are polluted, and for this reason, they are not used for irrigating crops in Kawkaba and the surrounding areas, while the olive trees are growing rainfed, as per what is indicated by the municipality of Kawkaba. Here as well, we did not find indication of direct Hg pollution.

Climatic data in both Bchaaleh and Kawkaba were collected from the meteorological station and manual rain gauge installed in the villages by LARI (Lebanese Agricultural Research Institute). CO_2 data used in this study are from NOAA Global Monitoring Laboratory (https://gml.noaa.gov/webdata/ccgg/trends/co2/co2_trend_gl.txt, last access: 10 January 2022).

2.2 Field sampling

For the Hg concentration analysis, four olive trees (3–5 m in diameter and an average height of 4–6 m) were sampled in each of the two groves from February 2019 to September 2020. Within Bchaaleh, two trees were selected from the upper terrace (BCO1 – Bchaaleh tree 1, BCO4 – Bchaaleh tree 4), and two other trees were sampled from a lower terrace located 1.5 m below the upper one (BCO9 – Bchaaleh tree 9, BCO12 – Bchaaleh tree 12; Fig. S2). In Kawkaba, four trees were selected and sampled (KWO1 – Kawkaba tree 1, KWO2 – Kawkaba tree 2, KWO3 – Kawkaba tree 3, KWO4 – Kawkaba tree 4). For each olive tree, both sun-exposed and shaded foliage and stems (terminal portions of 20 cm) with no evidence of pathogens were randomly taken and merged from the upper-, middle-, and lower-canopy positions of the olive trees on a monthly basis using a manual pruner. The phenological growth stages of olive trees described by Sanz-Cortés et al. (2002) in Spain suggest leaf development from March to November. Hence, it should be mentioned that the Hg concentration measured on monthly collected foliage represents an average of Hg accumulated in young foliage (year N of collection, where N is equal to 2019 and 2020) and older foliage (N-1 year and N-2 years). Fruits were collected in April 2019. Litter and soil surface were separately collected on the whole top surface area of the olive groves and stored in different paper bags once every 4 months. In parallel, soil sampling was performed using a bucket auger to a maximum depth of 60 cm. In both sites Bchaaleh and Kawkaba, the soil showed uniform color and texture. Soil cores were fractioned in the soil surface (0–1 cm), from 0 to 30 cm depth, and from 30 to 60 cm depth in order to study the effect and accumulation of Hg concentration on the different depth layers. To avoid contamination, gloves were worn while collecting samples, and the equipment were rinsed with methanol between every sample. A set of 453 samples was collected and stored in paper bags until further preparation for the Hg analysis.

2.3 Sample preparation for Hg analysis

Collected foliage and stems were rinsed with distilled water and then dried for 48 h in an oven at a temperature of 50 °C at maximum (Demers et al., 2013; Li et al., 2017; Pleijel et al., 2021). This procedure likely eliminated any Hg(0) present in the samples. The dried foliage, stems, litter, and olive fruits samples were ground using an electrical, stainless grinding machine with no heating system for 5–10 min, while soil samples were prepared with a manual natural-agate grinder. All samples were later sieved using an Inox stainless-steel 125-micron sieve mesh to collect homogeneous powders for analysis. A total of 150 mg for foliage and soil (50 mg per analysis), and 300 mg of litter and stems (100 mg per analysis) were considered in triplicates for analysis of Hg concentrations.

2.4 Analytical method

For the Hg elemental analysis, a total of 453 powder samples from foliage, stems, grain, litter, and soil were analyzed using an advanced Hg analyzer, AMA 254 (Altec), as described elsewhere (Barre et al., 2018; Duval et al., 2020). A known sample amount (50–100 mg) is weighed in a nickel boat using a 10^{-6} g precision balance. The sample aliquot is first dried at 120 °C for 60 s and subsequently pyrolyzed at 750 °C for 150 s under oxygen flow. The resulting gaseous Hg produced during the sample decomposition is amalgamated on a gold trap and then released to an atomic absorption spectrometer after a thermal desorption step at 950 °C. The AMA 254 instrument was calibrated through several external matrix-matched calibration procedures using the following certified reference materials: IAEA-456 sediment (77 ± 5 ng Hg g^{-1}), NIST-1575A pine needles ($39,9 \pm 0,7$ ng Hg g^{-1}), and IAEA336 (200 ± 40 ng Hg g^{-1}). The QA/QC evaluation of the analytical procedure was completed with a continuous monitoring of the blank's values (nickel-boat Hg background noise) every 15 analyzed samples. The precision of the measurements was assessed through replicated analyses ($n = 2$) of 13 % of the total amount of samples ($n = 453$). Average relative standard deviations of 5 % and 2.5 % are thus associated with the reported Hg concentrations for the 2019 and 2020 samples batches respectively. The absolute detection limit (ADL) of the analytical technique (AMA 254) was estimated at 0.04 ng Hg. As a consequence, the method detection limits (MDLs) for samples analyzed were 0.7 ng Hg g^{-1} for soil, litter, and foliage and 0.4 ng Hg g^{-1} for stems and wood. These MDLs were much lower than the measured Hg concentration in the various samples.

Subsamples of soil were used for carbon and nitrogen elemental contents (%) analysis; 2 mg (acid-washed soil and bulk soil) of powders were weighed into tin capsules and measured by dry combustion using a Pyrocube elemental analyzer (EA, Elementar GmbH).

2.5 Statistical analysis

For the statistical analysis, we used the R 4.1.0 program. Our data are not normally distributed, so for the effect of tissue type on Hg concentration, a Wilcoxon test was used with the tissue type (foliage and stems) as the main effect. Pearson correlation analysis was used to examine the inter-individual correlation of Hg concentration between the trees. Correlation between the Hg concentration of soil surface, litter, and foliage was studied using a correlation test. For the seasonal effect (winter: mid-December till mid-March; spring: mid-March till mid-June; summer: mid-June till mid-September; autumn: mid-September till mid-December) on Hg concentration, a Wilcoxon test was used, considering the unequal data available for the different seasons. Finally, the effect of climatic factors (temperature, precipitation, pCO_2) on Hg accumulation was examined using a Wilcoxon test.

3 Results

3.1 Hg concentrations in plant tissues, litter, and soil at Bchaaleh and Kawkaba groves

Hg concentrations measured in the different sampled materials (plant tissues, litter, and soil) varied generally according to both tree tissues and the groves' agro-climatic conditions (Table 1). Hg values in the foliage varied significantly between the two groves (p value $= 1.581 \times 10^{-6}$), where the highest concentration was recorded in Bchaaleh (48.1 ± 10.6 ng g^{-1}) vs. (35 ± 12.4 ng g^{-1}) in Kawkaba. Soil surface also demonstrated a difference in Hg concentration between Bchaaleh and Kawkaba, with 61.9 ± 20.0 ng g^{-1} in Bchaaleh and 128.5 ± 9.4 ng g^{-1} in Kawkaba. The values of the 0–30 cm soil samples taken from Bchaaleh and Kawkaba grove ranged between 31.8 ± 4.7 ng g^{-1} and 70.2 ± 23.4 ng g^{-1} respectively. In the 30–60 cm soil, Hg concentrations were recorded as 19.5 ± 6.73 ng g^{-1} at Bchaaleh. No significant differences were recorded for the litter and stems' Hg concentrations (p value $= 0.0915$ and p value $= 0.2215$ respectively) between the groves, with litter values of 62.9 ± 17.8 at Bchaaleh and 75.7 ± 20.3 ng g^{-1} at Kawkaba vs. stem values of 7.9 ± 2.8 ng g^{-1} at Bchaaleh and 9.0 ± 4.7 ng g^{-1} at Kawkaba. Positive correlations were observed between soil and litter in Bchaaleh ($r = 0.60$) and Kawkaba ($r = 0.95$), though these were statistically insignificant (p value $= 0.40$ and 0.13 respectively).

The comparison between Bchaaleh and Kawkaba soil surface Hg contents showed significant difference between the two groves (p value $= 0.04746$). We observe the same significant difference when comparing the soil horizon of the 0–30 cm layer of both groves. In descending order of Hg concentrations and considering the different sites, plant tissue, soil, and litter samples, the Hg concentrations could be ranked in Bchaaleh as follows: soil surface > litter > foliage

> soil 0–30 cm > soil 30–60 cm > stems > fruits; and in Kawkaba, soil surface > litter > soil 0–30> foliage > soil 30–60> stems > fruits (Table 1).

3.2 Seasonal variation of Hg concentration in plant tissues, litter, and soil

Hg concentrations recorded between February 2019 and September 2020 (Table 2) reflected a significant seasonal variation in both sites (p value $<2.2 \times 10^{-16}$)

In Bchaaleh grove, foliage registered its highest Hg concentrations during winter and spring, with 61.8 ± 7.6 ng g^{-1} and 55.1 ± 12.5 ng g^{-1} respectively, and its lowest Hg concentrations during summer and autumn, with 41.5 ± 12.7 ng g^{-1} and 44.4 ± 6.2 ng g^{-1} respectively. A seasonal effect on foliage and stems was registered (p value $<2.2 \times 10^{-16}$; Fig. 2a, c). The stems' and 0–30 cm soil's highest values were registered in autumn. Significant differences were found in foliage Hg values between summer and winter (p value $= 0.00020$) and between autumn and winter (p value $= 0.00014$). Similarly, stems Hg values varied significantly between spring and winter ($p$value $= 0.030$) and between autumn and winter ($p$value $= 0.047$). The highest litter Hg content occurred in summer in Bchaaleh olive groves (79.3 ± 26.5 ng g^{-1}), and the lowest occurred in winter (48.6 ± 13.3 ng g^{-1}; p value $= 0.2286$). The highest Hg contents in the soil surface of Bchaaleh was recorded in summer (84.5 ± 21.2 ng g^{-1}).

In Kawkaba, the highest Hg concentrations for foliage and stems were registered in spring with 51.8 ± 4.5 and 11.7 ± 6.7 ng g^{-1} respectively (Table 2, Fig. 2b, d). Significant differences were found in foliage Hg values between summer and winter (p value $= 0.013$), autumn and winter (p value $= 0.00067$), autumn and spring (p value $= 1.589 \times 10^{-5}$), spring and winter (p value $= 9.383 \times 10^{-5}$), and spring and summer (p value $= 2.327 \times 10^{-6}$). Similarly, stem Hg values varied significantly between spring and winter (p value $= 0.006$), spring and summer (p value $= 0.0036$), and autumn and spring (p value $= 0.011$). There is no seasonal variation between the litter in different seasons for either Bchaaleh or Kawkaba. Bchaaleh and Kawkaba groves soil surface, 0–30 cm, and 30–60 cm Hg values varied significantly between seasons (p value <0.05). A seasonal variation is observed in both olive groves, especially in the foliage.

3.3 Inter-individual variability between trees for each site

In the upper terrace of Bchaaleh grove, the average foliage Hg concentration of BCO4 and BCO1 varied between 42.4 ± 11.5 ng g^{-1} and 44.6 ± 13.3 ng g^{-1} respectively, showing no significant difference (p value $= 0.8225$). In the lower terrace of the same site, average foliage Hg concentrations of BCO12 and BCO9 were found to vary from 45.6 ± 12.7 to 60.7 ± 12.7 ng g^{-1} respectively (Fig. 2a), exhibiting a significant difference (p value $= 0.0059$). BCO9 is significantly different to each of the other three trees (p value <0.0059), while BCO1, BCO4, and BCO12 have very similar Hg contents (p value $= 0.46$).

In the upper terrace of Bchaaleh grove, the average stems Hg concentration of BCO4 and BCO1 varied between 7.0 ± 2.8 and 7.1 ± 2.9 ng g^{-1} respectively, showing no significant difference (p value $= 0.94$). In the lower terrace, average stems Hg concentrations of BCO12 and BCO9 were 6.4 ± 2.2 and 11.2 ± 5.2 ng g^{-1} respectively, showing a significant difference (p value $= 0.0054$; Fig. 2c). For BCO1 and BCO12, there was no significance difference (p value $= 0.5725$); the same goes for BCO4 and BCO12 (p value $= 0.523$).

The average concentrations per tree in foliage and stems were 32.4 ± 12.2 and 8.5 ± 4.0 ng g^{-1} respectively for KWO1, 32.8 ± 14.7 and 8.9 ± 6.0 ng g^{-1} for KWO2, 37.6 ± 14.0 and 9.3 ± 6.7 ng g^{-1} for KWO3, and 37.7 ± 13.6 and 9.6 ± 4.0 ng g^{-1} for KWO4 (Fig. 2b, d). In Kawkaba grove, comparison of the foliage Hg concentration between the four studied trees shows no significant difference ($0.22 < p$ value <1); this is also true for the stems ($0.21 < p$ value <0.96).

3.4 Hg concentration and agro-climatic effect

At first glance, seasonal variations of the Hg concentrations of the foliage of both sites suggest a covariation with climatic parameters (precipitation amounts, relative humidity, and temperature; Fig. S1) and atmospheric pCO_2. Foliage Hg content increased with higher precipitation and lower temperature (autumn and winter), while during the warmer and dryer seasons (May to mid-October), the Hg concentration of foliage decreased (Fig. S1). However, the Wilcoxon test for a non-normal distribution shows no significant correlation between Hg concentration of foliage and precipitation (p value $= 0.95$), while temperature, relative humidity, and atmospheric CO_2 (pCO_2) show a significant correlation value of 2.2×10^{-16}). For the stems, Hg concentration also showed no significant correlation with precipitation (p value $= 0.1147$) and a significant correlation with temperature, relative humidity, and pCO_2 (p value $= 2.2 \times 10^{-16}$).

4 Discussion

4.1 Hg concentration in plant tissues, soil, and litter in the studied groves

In both groves, our values showed a higher Hg concentration in the olive foliage (Bchaaleh average of 48.1 ± 10.6 ng g^{-1}; Kawkaba average of 35.0 ± 12.4 ng g^{-1}) than in the stems (Bchaaleh average of 7.9 ± 2.8 ng g^{-1}; Kawkaba average of 9.0 ± 4.7 ng g^{-1}) and in the olive fruits (7 ± 3.5 ng g^{-1} at Bchaaleh, $n = 3$ and 11 ng g^{-1} in Kawkaba, $n = 1$). Our data corroborate previous studies (Bargagli, 1995; Higueras et al., 2016) showing that olive foliage has the highest Hg concen-

Table 1. Overall mean values of Hg concentration (ng g^{-1}) of the different studied material in both Bchaaleh and Kawkaba olive groves.

Sample material	Bchaaleh (BC)			Kawkaba (KW)		
	Average (ng g^{-1})	SD	N	Average (ng g^{-1})	SD	N
Foliage	48.1	10.6	66	35.0	12.4	67
Stems	7.9	2.8	66	9.0	4.7	67
Litter	62.9	17.8	7	75.7	20.3	6
Soil surface	61.9	20.0	8	128. 5	9.4	6
Soil 0–30 cm	31.8	4.7	6	70.2	23.4	5
Soil 30–60 cm	19.5	6.7	5	28.0	–	1
Fruits	7.0	3.5	3	11.0	–	1

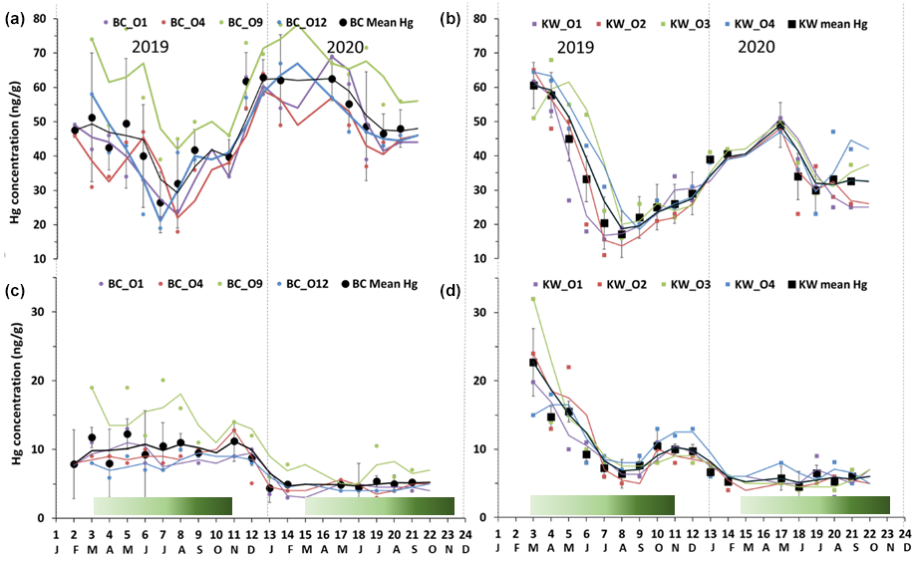

Figure 2. Seasonal variations of foliage Hg concentration in **(a)** Bchaaleh (BC) and **(b)** Kawkaba (KW) olive groves, and stems Hg concentration in **(c)** Bchaaleh and **(d)** Kawkaba olive groves. Shaded green horizontal bars represent the leaf development of olive trees during the growing season of cultivars in Spain according to the BBCH scale (Sanz-Cortès et al., 2002).

tration of plant tissues. Our values are lower than 200 ng g^{-1}, which is considered as the Hg pollution threshold (Kabata-Pendias and Pendias, 2000) and implies no pollution effect for either the Bchaaleh or Kawkaba groves (Table S2; Fig. S3a, b). This suggests that our sites are good remote bioindicators of the uptake of Hg through the plant, although a study with a more prolonged time range is needed. However, in an overview of vegetation uptake of mercury and its impacts on global cycling, Zhou et al. (2021) suggested lower values for unpolluted sites (litterfall 43 ng g^{-1} > foliage 20 ng g^{-1} and branch 12 ng g^{-1}). Knowing that our sites correspond to unpolluted areas of Lebanon and that the lower values of Zhou et al. (2021) were obtained from an ensemble of various species (trees and grasses) and not specifically from olive trees, we considered the threshold value of 200 ng g^{-1} (Kabata-Pendias and Pendias, 2000) to be more appropriate for our comparison.

As described in several studies, Hg in foliage originates predominantly from the atmospheric gaseous Hg(0) through stomatal uptake (Ericksen et al., 2003; Lindberg et al., 1979; Zhou et al., 2021). Adding to that, the Hg_{atm} uptake in foliage exceeds Hg stomatal re-emission (Pleijel et al., 2021; Zhou et al., 2021). Inside the leaves, the oxidized Hg(II) has high affinities for binding covalently with organic groups (Du and Fang, 1983; Clarkson and Magos, 2006; Pleijel et al., 2021). The Hg can be translocated by phloem transport to the stems and eventually into roots, and potential release into soils may also be contributing to Hg accumulation in soils (Giesler et al., 2017; Schaefer et al., 2020).

The soil surface and litter registered the highest Hg concentration (62 to 129 ng g^{-1}) among all samples (foliage, stems, fruit) in both groves (Table 1), suggesting that the soil is the main Hg reservoir through the Hg throughfall and litter inputs (Tomiyasu et al., 2005). Our findings are in agreement with studies on evergreen-forest ecosystems reporting

Table 2. Seasonal mean Hg concentration ($ng\,g^{-1}$) and standard deviations of the different studied materials in both Bchaaleh and Kawkaba olive groves. Bold formatting indicates the highest Hg concentration values among the different materials during the different seasons.

(a)	Hg ($ng\,g^{-1}$)											
Bchaaleh	Spring	SD	N	Summer	SD	N	Autumn	SD	N	Winter	SD	N
Foliage	**55.1**	**12.5**	**16**	41.5	12.7	24	44.4	6.2	12	**61.8**	**7.6**	**18**
Stems	7.8	3.8	16	7.61	3.9	24	**8.3**	**2.7**	**12**	6.4	2.9	18
Litter	**79.3**	**26.5**	**3**	64.7	4	4	55.5	3.54	2	48.6	13.3	3
Soil surface	58.3	13	3	**84.5**	**21.2**	**4**	50	–	1	50.6	23.5	3
0–30 cm	**33.6**	**6.2**	**2**	32.2	4.3	2	**34.5**	**7.79**	**2**	27	0.7	3
30–60 cm	**23.1**	**9.1**	**2**	20.7	10.32	2	19.6	9.05	2	11	–	1
(b)												
Kawkaba	Spring	SD	N	Summer	SD	N	Autumn	SD	N	Winter	SD	N
Foliage	**51.8**	**4.5**	**16**	28	7.2	24	28.5	7.2	16	33.9	5.6	18
Stems	**11.7**	**6.7**	**16**	6.5	1.4	24	7.7	2.1	16	6.9	1.6	18
Litter	**90.1**	**29.3**	**2**	67	24	2	70	1.4	2	–	–	–
Soil surface	**132**	**8.5**	**2**	118	4.2	2	**135.6**	**2.2**	**2**	–	–	–
0–30 cm	57.9	11.2	2	65.8	–	1	**84.8**	**36.4**	**2**	–	–	–
30–60 cm	28	–	1	–	–	–	–	–	–	–	–	–

that soil can hold more than 60 % of Hg input to the forest floor (Wang et al., 2016). Our soil surface site values ($61.9 \pm 20.0\,ng\,g^{-1}$ in Bchaaleh and $128.5 \pm 9.4\,ng\,g^{-1}$ in Kawkaba) show higher Hg concentration in Kawkaba compared to the general background level of Hg, as defined by uncontaminated-soil world reference mean Hg contents (20 to $100\,ng\,g^{-1}$; Kabata-Pendias and Pendias 2000; Senesil et al., 1999; Gworek et al., 2020). However, both sites have significantly lower values compared to known contaminated industrial and mining sites ($>1000\,ng\,g^{-1}$). Nevertheless, studies conducted at different sites show a wide range of natural background Hg levels (i.e., topsoils in Europe, India, Brazil, the Norwegian Arctic, and New Zealand have values of 40, 50, 80, 110, and $230\,ng\,g^{-1}$ respectively; Gworek et al., 2020), making it difficult to set a specific Hg threshold value for uncontaminated soil (Table S2 and Fig. S3c). Due to the differences registered in different countries and sites of sampled soil, this indicates a link with chemical and mineralogical soil properties (i.e., pH, humic acid, soil grain size distribution, organic matter type, and clay percentage) affecting Hg in soil and its transport (Richardson et al., 2013; Chen et al., 2016; O'Connor et al., 2019). Nitrogen can also be a factor affecting the Hg content in soil, depending on its characteristics. Nitrogen increase can change the equilibrium of the soil solution and the morphology of roots, causing a possible increase in Hg availability in soil and increasing the Hg uptake by the plant (Alloway, 1995; Barber, 1995; Carrasco-Gil et al., 2012). The increase in Hg availability in the soil is due to the organic nitrogen that provides a high absorption capacity, retaining the Hg_{atm} deposition (Obrist et al., 2009). Nitrogen supply prevents oxidative stress in roots but can also improve root development and increase the uptake of Hg from the soil (Carrasco-Gil et al., 2012). Hence, we suggest that lower values in Bchaaleh soils are likely explained by the low clay, organic carbon, and nitrogen contents (10.7 %, 4 %, and 0.3 % in the soil surface respectively), while Kawkaba's higher Hg soil contents can be explained by the higher clay proportion (66 %) and organic carbon and nitrogen contents (9 % and 0.92 %). On such clay loam soils and rich organic matter, Hg binding is facilitated, explaining the higher content (O'Connor et al., 2019).

The litter showed higher Hg concentration than foliage in both Bchaaleh ($62.9 \pm 17.8\,ng\,g^{-1}$) and Kawkaba ($75.7 \pm 20.3\,ng\,g^{-1}$; Table 1). This has been also described by Rea et al. (1996) and by Zhou et al. (2021) for uncontaminated and contaminated sites, where litterfall Hg contents were systematically higher than the foliage Hg contents. The bacterial and chemical decomposition of the litter significantly decrease the amount of C compared to the Hg that, conversely, may continue to increase due to the continued absorption of Hg from precipitation and throughfall (Obrist et al., 2011; Pokharel and Obrist, 2011; Zhou et al., 2021). Another possible explanation is that the leaves shed as litter are likely to mostly be the oldest leaves that have accumulated Hg over the longest period of time and that thus have, on average, higher Hg concentrations than the remaining foliage, since the latter consists of both younger and older foliage (Rea et al., 1996; Pleijel et al., 2021).

4.2 Seasonal foliage Hg content versus seasonal atmospheric Hg and CO_2

The late winter–early spring registered the highest Hg concentration for foliage in both groves, while summer and early

fall, to a lesser extent, recorded the lowest concentrations. This seasonal change is explained by the seasonal tree physiology variations, such as the Hg accumulation in leaves after stomatal uptake (Pleijel et al., 2021; Wohlgemuth et al., 2021). We can suggest that during winter–early spring, water is available, and photosynthetic activity is not limited; hence, both CO_2 and Hg diffuse through opened stomata inside the foliage. As shown in Fig. 2, Hg in foliage is low in summer–fall, and hence, the foliage acts as a sink of Hg. A clear seasonal pattern of Hg concentration in foliage is evident; despite being based on three generations of olive leaves (1–3 years old), with youngest leaves being known to have low concentrations (Pleijel et al., 2021), the seasonal signal is still very remarkable. Therefore, one can speculate that the mercury levels would have been higher if we had avoided the recently formed foliage during spring and early summer. This may also explain the large difference in Hg levels between litter and foliage.

Evergreen olive foliage at our sites showed a decrease in Hg contents from the end of March to late August, with minimum values centered in August, suggesting a decline of the plant Hg uptake that is likely explained by the reduction of the stomatal conductance (Lindberg et al., 2007; Pleijel et al., 2021). This minimal photosynthetic activity occurs during the driest season (0 mm precipitation) and the hottest temperatures (above 25 °C) at our sites. For the period 2018–2020, Martino et al. (2022) showed an atmospheric GEM depletion when NDVI (normalized difference vegetation index) values increased. This can explain the lower foliage Hg content in 2019 compared to that in 2020 at our study sites in Lebanon. This also collaborated the work of Jiskra et al. (2018) for the Northern Hemisphere site. Since no data of atmospheric mercury in Lebanon or surrounding countries are available, we used the Hg_{atm} time series data of Martino et al. (2022; Fig. 3a). We observed opposite trends between foliage Hg concentration and air Hg concentration (negative covariation in 2019 and positive covariation in 2020; Fig. a, d, e).

Alternatively, other studies reported a positive correlation between Hg_{atm} and crops (Niu et al., 2011), as observed in our study between the Hg foliage and the Hg_{atm} in 2020 (Fig. 3a, d, e). This supports the hypothesis that, where our groves are seasonally exposed to high Hg_{atm}, they accumulate Hg in their foliage (Lindberg et al., 2007; Pleijel et al., 2021). According to Hanson et al. (1995), a compensation point for Hg uptake by plant foliage can be considered, but no information, to our knowledge, is available for the specific case of the olive trees. The tight link between foliage Hg uptake and stomatal-conductance seasonal variations can be also deduced from the analysis of the partial pressure of the atmospheric pCO_2 (pCO_{2atm}) seasonal variation (Obrist, 2007; Jiskra et al., 2018; Obrist et al., 2018; Pleijel et al., 2021) (Fig. 3b, d, e). Very good covariation between olive foliage Hg and pCO_{2atm} are shown for Bchaaleh and Kawkaba, despite the fact that a notable offset of 1 month at Kawkaba to 2 months at Bchaaleh can be deduced (Fig. S4). Taking into account our calculated time lags, we obtained significant correlations between our foliage Hg content and pCO_{2atm} of 0.718 and 0.704 in Bchaaleh and Kawkaba respectively. Interestingly, a 1-month time lag between Hg_{atm} and pCO_{2atm} is also reported by Jiskra et al. (2018) for most Northern Hemisphere sites. The offset of 1 to 2 months between the maxima of Bchaaleh and Kawkaba foliage Hg (March and April) and pCO_{2atm} (May) suggests that the minimum of Hg in the foliage occurs during the decreasing phase of the pCO_{2atm}, when the global Northern Hemisphere tends to become a net sink of CO_2. When minimum values of pCO_{2atm} are reached at the end of the dry summer (Fig. 3b), with concomitant to minimum Hg_{atm} (Fig. 3a) and the end of the drought and an increase of precipitation (Fig. 3c), Bchaleh and Kawkaba olive trees show a recovery in the Hg uptake rates. The photosynthetic activity and the stomatal conductance related to the climatic parameters (temperature, precipitation, humidity, pCO_2), as shown by Ozturk et al. (2021), and the Hg_{atm} explain our foliage Hg seasonal cycle. At a regional scale, our sites show different time lags between Bchaaleh and Kawkaba that we cannot explain fully apart from their altitudinal differences, which can suggest that Bchaaleh grove benefits from less drought in summer.

4.3 Hg cycling in the stems, litter, and soil system

For each site, Hg content in stems exhibits a narrow range between the different trees, except for tree BCO9, which had the highest stem values. We speculate that this higher Hg content is the adjunction of chemical products such as fertilizer on the plot 549, which belongs to a different owner (Fig. S2), likely between fall and winter. It was observed by Zhao and Wang (2010) that the fertilizer used and its source of phosphorous may affect the Hg content in the product and thus affect the amount of Hg transported into the fertilized soil.

At a seasonal scale, the averaged Hg values of the soil system show statistically significant differences between the four seasons, while those of the stems show statistically significant differences between winter (lowest values) and spring (p value $= 0.030$) and winter–autumn (p value $= 0.047$) in Bchaaleh grove, mostly similar to foliage changes, while litter shows no significant difference between seasons. The same behavior was registered in Kawkaba in the litter and soils, while stems showed statistically significant differences between autumn and spring (p value $= 0.011$), spring–winter (p value $= 0.006$), and spring–summer (p value $= 0.004$; Table 2). Despite the small amount of Hg content in the stems, the statistically significant seasonal changes may suggest that small amounts of Hg move from the foliage to the lignified tissues such as the stems. However, we cannot neglect the Hg transport in the xylem sap from the roots to the aboveground plant tissues, even if it is minimal (Yang et al., 2018).

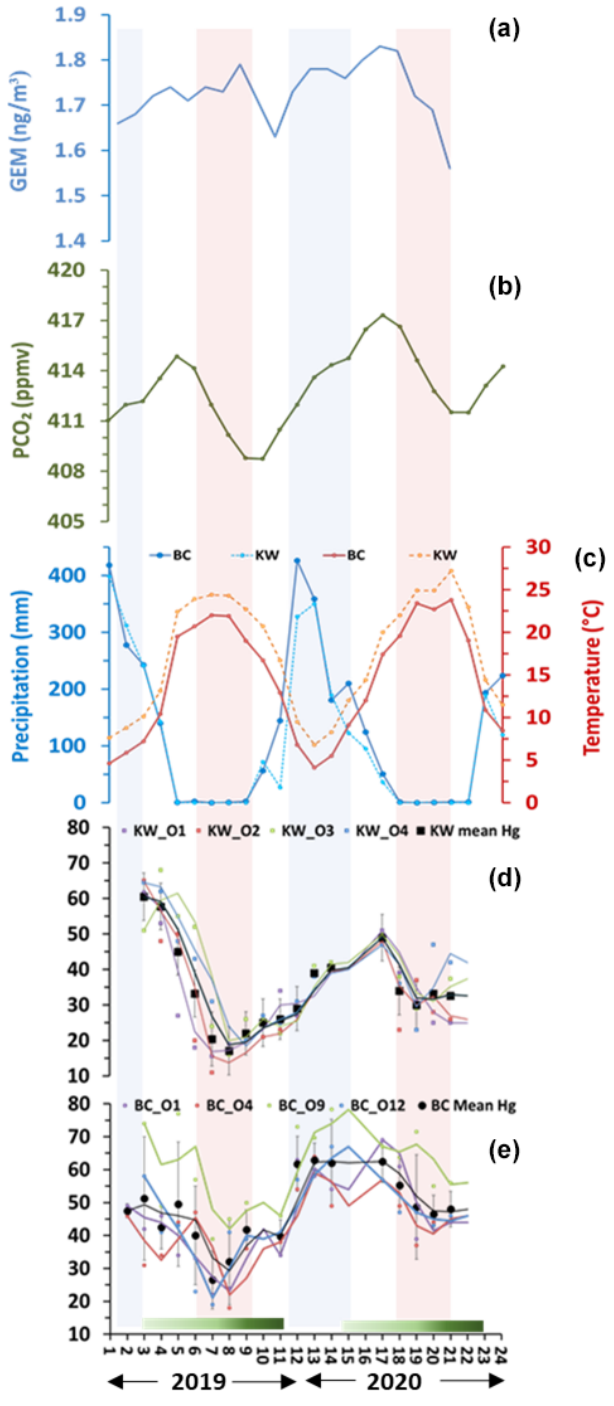

Figure 3. Seasonal variations of **(a)** atmospheric Hg(0) (Martino et al., 2022), **(b)** pCO_2 (NOAA Global Monitoring Laboratory), **(c)** precipitation and temperature of Bchaaleh and Kawkaba respectively, and **(d)** and **(e)** foliage Hg concentration in Bchaaleh and Kawkaba olive groves respectively. Shaded green horizontal bars represent the leaf development of olive trees during the growing season of cultivars in Spain according to the BBCH scale (Sanz-Cortès et al., 2002). Shaded colored lines correspond to the winter (blue) and summer (red).

We can suggest the following Hg cycling in the system of the olive grove's soil. In winter–early spring, the highest concentrations in foliage continuously feed the litter and can explain the following maximal spring Hg content of the litter. The decomposition of the litter organic matter during the wettest conditions likely liberates Hg in the Hg(0) or Hg(II) forms or MeHg, either towards the atmosphere or the surface soil (see Table 2) respectively (Gworek et al., 2020). A fraction of the degraded organic matter is transferred through gaseous evaporative processes towards the atmosphere, while another fraction of the Hg leaches towards the deeper soil in addition to dry Hg deposition during the dry season (Teixeira et al., 2017). We can also speculate that the small Hg decrease observed in the 0–30 cm and 30–60 cm during the winter season in Bchaaleh could be due to the minimal absorption of total Hg and MeHg through the roots and xylem sap to the above-ground tissues (Johnson and Lindberg, 1995).

5 Conclusions

This is the first study conducted on monumental olive trees in a remote site of the MENA region without local contamination and followed on a monthly basis over 18 months. Findings of our study indicate a higher uptake of Hg in the olive foliage compared to in stems and fruit items and a remarkable Hg foliage seasonal variation in both studied groves. Winter and spring were particularly suitable for Hg accumulation in foliage at both sites. The significant correlation between our Hg foliage contents and the Hg_{atm} content and pCO_2, despite the 1-to-2-month time lag, suggests that the main source of Hg foliage is the Hg_{atm}, as observed in different species and studies (conifers and hardwood). Hg is absorbed by the foliage via the open stomata, driven by the interaction of high vegetal activity, temperature, water availability, and the processes that control transpiration, which are likely to be seasonal. Hence, physiological and climatic processes explain the seasonal Hg accumulation in foliage. Thus, a more intensive study taking account of the phenological dynamics of olive tree foliage must be focused on. Further comparison and studies on the seasonal Hg_{atm} in the eastern Mediterranean basin are necessary to test our hypothesis of the reversed seasonality of Hg in 2019 and the positive covariation in 2020, since, contrary to the global Northern Hemisphere and western Mediterranean region's vegetation, our olive groves act as a sink of Hg and CO_2 when global Northern Hemisphere and western Mediterranean vegetation is emitting. This relationship of Hg of foliage–atmospheric Hg–atmospheric pCO_2 should be further investigated along the season and locally to better understand the observed time lags. Soil surface registered the highest Hg concentration among all studied compartments due to well-known processes of litter and throughfall that incorporate Hg to the soil surface. Moreover, this study highlights significant dif-

ferences between Hg of soil in the Bchaaleh and Kawkaba groves due to differences in the soil characteristics. In this study, we worked on the present time samples in order to have a better understanding of the Hg cycle in the olive trees. Our main contribution in this study is to see how the present-day olive trees record some elements such as Hg to better understand how the Hg in tree rings could be used for the past accumulation records.

Data availability. The datasets generated and/or analyzed during the current study are available from the corresponding author upon reasonable request.

Supplement. The supplement related to this article is available online at: https://doi.org/10.5194/bg-20-619-2023-supplement.

Author contributions. The corresponding author, IB, was responsible for ensuring that the descriptions were accurate and agreed upon by all authors. Conceptualization and methodology were done and developed by IB and LC. The material collection was performed by NT, IB, LC, IJ, and MER. Sample storage and preparation in Lebanon were organized by NT. Material preparation at ISEM was conducted by NT. Data collection and analysis were performed by NT, IB, DA, and ET. The setting of the meteorological stations was conducted by IJ. Subsamples of soil were analyzed for carbon and nitrogen elemental contents (%) by FF. The first draft of the paper was written by NT. IB, LC, DA, IJ, and MER commented on previous versions of the paper. All authors read and approved the final paper. Supervision was done by IB and LC.

Competing interests. The contact author has declared that none of the authors has any competing interests.

Disclaimer. Publisher's note: Copernicus Publications remains neutral with regard to jurisdictional claims in published maps and institutional affiliations.

Acknowledgements. The Institute of Evolutionary Science of Montpellier (ISEM) at Montpellier University and the Research Platform for Environment and Science – Doctoral School of Science and Technology (PRASE-EDST) at the Lebanese University are acknowledged for their support of the laboratory work. Credits go to the Lebanese Agriculture Research Institute (LARI) for assuring automated weather stations and manual rain gauges per site. The authors are grateful to the Municipality of Bchaaleh (Rachid Geagea) and the Municipality of Kawkaba (Mira Khoury). Acknowledgments are extended to Amira Yousef at LARI for her kind support and to Akram Tabaja for helping during fieldwork. We are very grateful to Hakan Pleijel, who reviewed this article, improving significantly our paper. We deeply acknowledge Andrew Johnston for the English revision.

Financial support. This work was supported by the National Council for Scientific Research of Lebanon (CNRS-L), Montpellier University doctoral fellowship grant (CNRS-L/UM), and the Franco-Lebanese Hubert Curien Partnership (PHC-CEDRE; project no. 44559PL).

Review statement. This paper was edited by Jens-Arne Subke and reviewed by Håkan Pleijel and three anonymous referees.

References

Abou Habib, N., Taleb, M., and Khoury, R.: Environmental and social safeguard studies for lake qaraoun pollution prevention project, V1(E4749), https://www.cdr.gov.lb/getmedia/6de7234e-c929-4625-887c-d8dfff87bea3/2015-01-29-Qaraoun-ESMF_issued-for-distribution.pdf.aspx (last access: 11 October 2021), 2015.

Alcaras, L. M. A., Rousseaux, M. C., and Searles, P. S.: Responses of several soil and plant indicators to post-harvest regulated deficit irrigation in olive trees and their potential for irrigation scheduling, Agr. Water Manage., 171, 10–20, https://doi.org/10.1016/j.agwat.2016.03.006, 2016.

Alloway, B. J.: Heavy Metals in Soils, Trace Metals and Metalloids in Soils and their Bioavailability, in: Environmental Pollution, Springer Science & Business Media, Blackie Academic & Professional, an imprint of Chapman & Hall, Glasgow, UK, ISBN 0751401986, https://link.springer.com/book/10.1007/978-94-007-4470-7 (last access: 30 November 2022), 1995.

Al-Zubaidi, A., Yanni, S., and Bashour, I.: Potassium status in some Lebanese soils, Lebanese Science Journal, 9, 81–97, 2008.

Assad, M.: Transfert des éléments traces métalliques vers les végétaux: mécanismes et évaluations des risques dans des environnements exposés à des activités anthropiques, Sciences agricoles, Université Bourgogne Franche-Comté, France, 218, NNT: 2017UBFCD006, 2017.

Baayoun, A., Itani, W., El Helou, J., Halabi, L., Medlej, S., El Malki, M., Moukhadder, A., Aboujaoude, L. K., Kabakian, V., Mounajed, H., Mokalled, T., Shihadeh, A., Lakkis, I., and Saliba, N. A.: Emission inventory of key sources of air pollution in Lebanon, Atmos. Environ., 215, 116871, https://doi.org/10.1016/j.atmosenv.2019.116871, 2019.

Badr, R., Holail, H., and Olama, Z.: Water quality assessment of hasbani river in south lebanon: microbiological and chemical characteristics and their impact on the ecosystem, J. Global Biosci., 3, 536–551, https://www.mutagens.co.in/jgb/vol.03/2/19.pdf, (last access: 11 October 2021), 2014.

Barber, S. A.: Soil Nutrient Bioavailability: A Mechanistic Approach, John Wiley and Sons, 432 pp., ISBN 9780471587477, 1995.

Bargagli, R.: The elemental composition of vegetation and the possible incidence of soil contamination of samples, Sci. Total Environ., 176, 121–128, https://doi.org/10.1016/0048-9697(95)04838-3, 1995.

Barre, J. P. G., Deletraz, G., Sola-Larrañaga, C., Santamaria, J. M., Bérail, S., Donard, O. F. X., and Amouroux, D.: Multi-element isotopic signature (C, N, Pb, Hg) in epiphytic lichens to discriminate atmospheric contamina-

tion as a function of land-use characteristics (Pyrénées-Atlantiques, SW France), Environ. Pollut., 243, 961–971, https://doi.org/10.1016/j.envpol.2018.09.003, 2018.

Beauford, W., Barber, J., and Barringer, A. R.: Uptake and Distribution of Mercury within Higher Plants, Physiologia Plantarum, 39, 261–265, https://doi.org/10.1111/j.1399-3054.1977.tb01880.x, 1977.

Besnard, G., Khadari, B., Navascues, M., Fernandez-Mazuecos, M., Bakkali, A. E., Arrigo, N., Baali-Cherif, D., de Caraffa, V. B.-B., Santoni, S., Vargas, P., and Savolainen, V.: The complex history of the olive tree: From Late Quaternary diversification of Mediterranean lineages to primary domestication in the northern Levant, P. Roy. Soc. B-Biol. Sci., 280, 1593, https://doi.org/10.1098/rspb.2012.2833, 2013.

Bishop, K. H., Lee, Y.-H., Munthe, J., and Dambrine, E.: Xylem sap as a pathway for total mercury and methylmercury transport from soils to tree canopy in the boreal forest, Biogeochemistry, 40, 101–113, https://doi.org/10.1023/A:1005983932240, 1998.

Bishop, K., Shanley, J. B., Riscassi, A., de Wit, H. A., Eklöf, K., Meng, B., Mitchell, C., Osterwalder, S., Schuster, P. F., Webster, J., and Zhu, W.: Recent advances in understanding and measurement of mercury in the environment: Terrestrial Hg cycling, Sci. Total Environ., 721, 137647, https://doi.org/10.1016/j.scitotenv.2020.137647, 2020.

Blackwell, B. D. and Driscoll, C. T.: Using foliar and forest floor mercury concentrations to assess spatial patterns of mercury deposition, Environ. Pollut., 202, 126–134, https://doi.org/10.1016/j.envpol.2015.02.036, 2015.

Boening, D. W.: Ecological effects, transport, and fate of mercury: A general review, Chemosphere, 40, 1335–1351, https://doi.org/10.1016/s0045-6535(99)00283-0, 2000.

Borjac, J., El Joumaa, M., Kawach, R., Youssef, L., and Blake, D. A.: Heavy metals and organic compounds contamination in leachates collected from Deir Kanoun Ras El Ain dump and its adjacent canal in South Lebanon, Heliyon, 5, e02212, https://doi.org/10.1016/j.heliyon.2019.e02212, 2019.

Borjac, J., El Joumaa, M., Youssef, L., Kawach, R., and Blake, D. A.: Quantitative Analysis of Heavy Metals and Organic Compounds in Soil from Deir Kanoun Ras El Ain Dump, Lebanon, Sci. World J., 2020, 1–10, https://doi.org/10.1155/2020/8151676, 2020.

Briffa, J., Sinagra, E., and Blundell, R.: Heavy metal pollution in the environment and their toxicological effects on humans, Heliyon, 6, e04691, https://doi.org/10.1016/j.heliyon.2020.e04691, 2020.

Carrasco-Gil, S., Estebaranz-Yuberob, M., Medel-Cuestab, D., Millán, R., and Hernández, L. E.: Influence of nitrate fertilization on Hg uptake and oxidative stress parameters in alfalfa plants cultivated in a Hg-polluted soil, Environ. Exp. Bot., 75, 16–24, https://doi.org/10.1016/j.envexpbot.2011.08.013, 2012.

Cavallini, A., Natali, L., Durante, M., and Maserti, B.: Mercury uptake, distribution and DNA affinity in durum wheat (Triticum durum Desf.) plants, Sci. Total Environ., 243–244, 119–127, https://doi.org/10.1016/S0048-9697(99)00367-8, 1999.

Chen, X., Ji, H., Yang, W., Zhu, B., and Ding, H.: Speciation and distribution of mercury in soils around gold mines located upstream of Miyun Reservoir, Beijing, China, J. Geochem. Explor., 163, 1–9, https://doi.org/10.1016/j.gexplo.2016.01.015, 2016.

Clarkson, T. W. and Magos, L.: The Toxicology of Mercury and Its Chemical Compounds, Crit. Rev. Toxicol., 36, 609–662, https://doi.org/10.1080/10408440600845619, 2006.

Dastoor, A., Angot, H., Bieser, J., Christensen, J. H., Douglas, T. A., Heimbürger-Boavida, L.-E., Jiskra, M., Mason, R. P., McLagan, D. S., Obrist, D., Outridge, P. M., Petrova, M. V., Ryjkov, A., St. Pierre, K. A., Schartup, A. T., Soerensen, A. L., Toyota, K., Travnikov, O., Wilson, S. J., and Zdanowicz, C.: Arctic mercury cycling, Nat. Rev. Earth Environ., 3, 4, https://doi.org/10.1038/s43017-022-00269-w, 2022.

Demers, J. D., Blum, J. D., and Zak, D. R.: Mercury isotopes in a forested ecosystem: Implications for air-surface exchange dynamics and the global mercury cycle: Mercury isotopes in a forested ecosystem, Global Biogeochem. Cy., 27, 222–238, https://doi.org/10.1002/gbc.20021, 2013.

Du, S.-H. and Fang, S. C.: Catalase activity of C3 and C4 species and its relationship to mercury vapor uptake Environ. Exp. Bot., 23, 347–353, https://doi.org/10.1016/0098-8472(83)90009-6, 1983.

Duval, B., Gredilla, A., Fdez-Ortiz de Vallejuelo, S., Tessier, E., Amouroux, D., and De Diego, A.: A simple determination of trace mercury concentrations in natural waters using dispersive Micro-Solid phase extraction preconcentration based on functionalized graphene nanosheets, Microchem. J., 154, 104549, https://doi.org/10.1016/j.microc.2019.104549, 2020.

EJOLT: Cimenterie Nationale Factory in Chekaa, Lebanon, EJAtlas, Environmental Justice Atlas, ejatlas [data set], https://ejatlas.org/conflict/chekaa, last access: 11 September 2019.

Ericksen, J. A., Gustin, M. S., Schorran, D. E., Johnson, D. W., Lindberg, S. E., and Coleman, J. S.: Accumulation of atmospheric mercury in forest foliage, Atmos. Environ., 37, 1613–1622, https://doi.org/10.1016/S1352-2310(03)00008-6, 2003.

Ermolin, M. S., Fedotov, P. S., Malik, N. A., and Karandashev, V. K.: Nanoparticles of volcanic ash as a carrier for toxic elements on the global scale, Chemosphere, 200, 16–22, https://doi.org/10.1016/j.chemosphere.2018.02.089, 2018.

Friedli, H. R., Arellano, A. F., Cinnirella, S., and Pirrone, N.: Initial Estimates of Mercury Emissions to the Atmosphere from Global Biomass Burning, Environ. Sci. Technol., 43, 3507–3513, https://doi.org/10.1021/es802703g, 2009.

Galatali, S., A., N. and Kaya, E.: Characterization of Olive (Olea Europaea L.) Genetic Resources via PCR-Based Molecular Marker Systems, European Journal of Biology & Biotechnology, 2, 26–33, https://doi.org/10.24018/ejbio.2021.2.1.146, 2021.

Gårdfeldt, K., Sommar, J., Ferrara, R., Ceccarini, C., Lanzillotta, E., Munthe, J., Wängberg, I., Lindqvist, O., Pirrone, N., Sprovieri, F., Pesenti, E., and Strömberg, D.: Evasion of mercury from coastal and open waters of the Atlantic Ocean and the Mediterranean Sea, Atmos. Environ., 37, 73–84, https://doi.org/10.1016/S1352-2310(03)00238-3, 2003.

Gérard, J. and Nehmé, C.: Lebanon, Méditerranée, Revue Géographique Des Pays Méditerranéens, Journal of Mediterranean Geography, 131, 131, https://doi.org/10.4000/mediterranee.11018, 2020.

Giesler, R., Clemmensen, K. E., Wardle, D. A., Klaminder, J., and Bindler, R.: Boreal Forests Sequester Large Amounts of Mercury over Millennial Time Scales in the Absence of Wildfire, Environ. Sci. Technol., 51, 2621–2627, https://doi.org/10.1021/acs.est.6b06369, 2017.

Grigal, D.: Mercury Sequestration in Forests and Peatlands: A Review, J. Environ. Qual., 32, 393–405, https://doi.org/10.2134/jeq2003.0393, 2003.

Guarino, F., Improta, G., Triassi, M., Castiglione, S., and Cicatelli, A.: Air quality biomonitoring through Olea europaea L.: The study case of "Land of pyres", Chemosphere, 282, 131052, https://doi.org/10.1016/j.chemosphere.2021.131052, 2021.

Gworek, B., Dmuchowski, W., and Baczewska-Dąbrowska, A. H.: Mercury in the terrestrial environment: A review, Environmental Sciences Europe, 32, 128, https://doi.org/10.1186/s12302-020-00401-x, 2020.

Hanson, P. J., Lindberg, S. E., Tabberer, T. A., Owens, J. G., and Kim, K.-H.: Foliar exchange of mercury vapor: Evidence for a compensation point, Water Air Soil Pollut., 80, 373–382, https://doi.org/10.1007/BF01189687, 1995.

Higueras, P., Amorós, J. A., Esbrí, J. M., García-Navarro, F. J., Pérez de los Reyes, C., and Moreno, G.: Time and space variations in mercury and other trace element contents in olive tree leaves from the Almadén Hg-mining district, J. Geochem. Explor., 123, 143–151, https://doi.org/10.1016/j.gexplo.2012.04.012, 2012.

Higueras, P. L., Amorós, J. Á., Esbrí, J. M., Pérez-de-los-Reyes, C., López-Berdonces, M. A., and García-Navarro, F. J.: Mercury transfer from soil to olive trees, A comparison of three different contaminated sites, Environ. Sci. Pollut. Res., 23, 6055–6061, https://doi.org/10.1007/s11356-015-4357-2, 2016.

Jiskra, M., Sonke, J. E., Obrist, D., Bieser, J., Ebinghaus, R., Myhre, C. L., Pfaffhuber, K. A., Wängberg, I., Kyllönen, K., Worthy, D., Martin, L. G., Labuschagne, C., Mkololo, T., Ramonet, M., Magand, O., and Dommergue, A.: A vegetation control on seasonal variations in global atmospheric mercury concentrations, Nat. Geosci., 11, 244–250, https://doi.org/10.1038/s41561-018-0078-8, 2018.

Johnson, and Lindberg: The biogeochemical cycling of Hg in forests: Alternative methods for quantifying total deposition and soil emission, Water Air Soil Pollut., 80, 1069–1077, 1995.

Jurdi, M., Korfali, S. I., Karahagopian, Y., and Davies, B. E.: Evaluation of Water Quality of the Qaraaoun Reservoir, Lebanon: Suitability for Multipurpose Usage, Kluwer Academic Publishers, The Netherlands, Environmental Monitoring and Assessment, 77, 11–30, 2002.

Kabata-Pendias, A. and Pendias, H.: Trace elements in soils and plants (3rd edn.), CRC Press, ISBN 0849315751, 2000.

Khadari, B., El Bakkali, A., Essalouh, L., Tollon, C., Pinatel, C., and Besnard, G.: Cultivated Olive Diversification at Local and Regional Scales: Evidence From the Genetic Characterization of French Genetic Resources, Front. Plant Sci., 10, 1593, https://doi.org/10.3389/fpls.2019.01593, 2019.

Khatib, J. M., Baydoun, S., and ElKordi, A. A.: Water Pollution and Urbanisation Trends in Lebanon: Litani River Basin Case Study, in: Urban Pollution: Science and Management, edited by: Charlesworth, S. M. and Booth, C. A., John Wiley & Sons Ltd., 397–415, https://doi.org/10.1002/9781119260493.ch30, 2018.

Kobrossi, R., Nuwayhid, I., Sibai, A. M., El-Fadel, M., and Khogali, M.: Respiratory health effects of industrial air pollution on children in North Lebanon, Int. J. Environ. Heal. R., 12, 205–220, https://doi.org/10.1080/09603/202/000000970, 2002.

Kotnik, J., Sprovieri, F., Ogrinc, N., Horvat, M., and Pirrone, N.: Mercury in the Mediterranean, part I: Spatial and temporal trends, Environ. Sci. Pollut. Res., 21, 4063–4080, https://doi.org/10.1007/s11356-013-2378-2, 2014.

Labdaoui, D., Lotmani, B., and Aguedal, H.: Assessment of Metal Pollution on the Cultivation of Olive Trees in the Petrochemical Industrial Zone of Arzew (Algeria), South Asian Journal of Experimental Biology, 11, 3, https://doi.org/10.38150/sajeb.11(3).p227-233, 2021.

Li, D., Fang, K., Li, Y., Chen, D., Liu, X., Dong, Z., Zhou, F., Guo, G., Shi, F., Xu, C., and Li, Y.: Climate, intrinsic water-use efficiency and tree growth over the past 150 years in humid subtropical China, PLOS ONE, 12, e0172045, https://doi.org/10.1371/journal.pone.0172045, 2017.

Li, R., Wu, H., Ding, J., Fu, W., Gan, L., and Li, Y.: Mercury pollution in vegetables, grains and soils from areas surrounding coal-fired power plants, Sci. Rep., 7, 46545, https://doi.org/10.1038/srep46545, 2017.

Lindberg, S., Bullock, R., Ebinghaus, R., Engstrom, D., Feng, X., Fitzgerald, W., Pirrone, N., Prestbo, E., and Seigneur, C.: A Synthesis of Progress and Uncertainties in Attributing the Sources of Mercury in Deposition, Ambio, 36, 19–32, 2007.

Lindberg, S. E., Jackson, D. R., Huckabee, J. W., Janzen, S. A., Levin, M. J., and Lund, J. R.: Atmospheric Emission and Plant Uptake of Mercury from Agricultural Soils near the Almadén Mercury Mine, J. Environ. Qual., 8, 572–578, https://doi.org/10.2134/jeq1979.00472425000800040026x, 1979.

Lodenius, M., Tulisalo, E., and Soltanpour-Gargari, A.: Exchange of mercury between atmosphere and vegetation under contaminated conditions, Sci. Total Environ., 304, 169–174, https://doi.org/10.1016/S0048-9697(02)00566-1, 2003.

Luo, Y., Duan, L., Driscoll, C. T., Xu, G., Shao, M., Taylor, M., Wang, S., and Hao, J.: Foliage/atmosphere exchange of mercury in a subtropical coniferous forest in south China, J. Geophys. Res.-Biogeosci., 121, 2006–2016, https://doi.org/10.1002/2016JG003388, 2016.

Maillard, F., Girardclos, O., Assad, M., Zappelini, C., Pérez Mena, J. M., Yung, L., Guyeux, C., Chrétien, S., Bigham, G., Cosio, C., and Chalot, M.: Dendrochemical assessment of mercury releases from a pond and dredged-sediment landfill impacted by a chlor-alkali plant, Environ. Res., 148, 122–126, https://doi.org/10.1016/j.envres.2016.03.034, 2016.

Martino, M., Tassone, A., Angiuli, L., Naccarato, A., Dambruoso, P. R., Mazzone, F., Trizio, L., Leonardi, C., Petracchini, F., Sprovieri, F., Pirrone, N., D'Amore, F., and Bencardino, M.: First atmospheric mercury measurements at a coastal site in the Apulia region: Seasonal variability and source analysis, Environ. Sci. Pollut. Res., 29, 68460–68475, https://doi.org/10.1007/s11356-022-20505-6, 2022.

McLagan, D. S., Stupple, G. W., Darlington, A., Hayden, K., and Steffen, A.: Where there is smoke there is mercury: Assessing boreal forest fire mercury emissions using aircraft and highlighting uncertainties associated with upscaling emissions estimates, Atmos. Chem. Phys., 21, 5635–5653, https://doi.org/10.5194/acp-21-5635-2021, 2021.

McLagan, D. S., Biester, H., Navrátil, T., Kraemer, S. M., and Schwab, L.: Internal tree cycling and atmospheric archiving of mercury: examination with concentration and stable isotope analyses, Biogeosciences, 19, 4415–4429, https://doi.org/10.5194/bg-19-4415-2022, 2022.

Naharro, R., Esbri, J., Amorós, J., and Higueras, P.: Atmospheric mercury uptake and desorption from olive-tree leaves, EGU General Assembly Conference Abstracts, Proceedings from the conference, EGU General Assembly 2018, 4–13 April 2018, Vienna, Austria, Geophysical Research Abstracts, 20, 2982, https://www.researchgate.net/publication/324169906 (last access: 11 June 2021), 2018.

Nassif, N., Jaoude, L. A., El Hage, M., and Robinson, C. A.: Data Exploration and Reconnaissance to Identify Ocean Phenomena: A Guide for In Situ Data Collection, J. Water Res. Protect., 8, 929–943, https://doi.org/10.4236/jwarp.2016.810076, 2016.

Niu, Z., Zhang, X., Wang, Z., and Ci, Z.: Field controlled experiments of mercury accumulation in crops from air and soil, Environ. Pollut., 159, 2684–2689, https://doi.org/10.1016/j.envpol.2011.05.029, 2011.

Obrist, D.: Atmospheric mercury pollution due to losses of terrestrial carbon pools?, Biogeochemistry, 85, 119–123, https://doi.org/10.1007/s10533-007-9108-0, 2007.

Obrist, D., Johnson, D. W., and Lindberg, S. E.: Mercury concentrations and pools in four Sierra Nevada forest sites, and relationships to organic carbon and nitrogen, Biogeosciences, 6, 765–777, https://doi.org/10.5194/bg-6-765-2009, 2009.

Obrist, D., Kirk, J. L., Zhang, L., Sunderland, E. M., Jiskra, M., and Selin, N. E.: A review of global environmental mercury processes in response to human and natural perturbations: Changes of emissions, climate, and land use, Ambio, 47, 116–140, https://doi.org/10.1007/s13280-017-1004-9, 2018.

Obrist, D., Johnson, D. W., Lindberg, S. E., Luo, Y., Hararuk, O., Bracho, R., Battles, J. J., Dail, D. B., Edmonds, R. L., Monson, R. K., Ollinger, S. V., Pallardy, S. G., Pregitzer, K. S., and Todd, D. E.: Mercury Distribution Across 14 U.S. Forests, Part I: Spatial Patterns of Concentrations in Biomass, Litter, and Soils, Environ. Sci. Technol., 45, 3974–3981, https://doi.org/10.1021/es104384m, 2011.

O'Connor, D., Hou, D., Ok, Y. S., Mulder, J., Duan, L., Wu, Q., Wang, S., Tack, F. M. G., and Rinklebe, J.: Mercury speciation, transformation, and transportation in soils, atmospheric flux, and implications for risk management: A critical review, Environ. Int., 126, 747–761, https://doi.org/10.1016/j.envint.2019.03.019, 2019.

Ozturk, M., Altay, V., Gönenç, T. M., Unal, B. T., Efe, R., Akçiçek, E., and Bukhari, A.: An Overview of Olive Cultivation in Turkey: Botanical Features, Eco-Physiology and Phytochemical Aspects, Agronomy, 11, 295, https://doi.org/10.3390/agronomy11020295, 2021.

Patra, M. and Sharma, A.: Mercury toxicity in plants, The Botanical Review, 66, 379–422, https://doi.org/10.1007/BF02868923, 2000.

Petrlik, J., Kodeih, N., IndyACT, Arnika Association, and IPEN WG.: Mercury in Fish and Hair Samples from Batroun, Lebanon, https://doi.org/10.13140/RG.2.2.12052.40327, 2013.

Pleijel, H., Klingberg, J., Nerentorp, M., Broberg, M. C., Nyirambangutse, B., Munthe, J., and Wallin, G.: Mercury accumulation in leaves of different plant types – the significance of tissue age and specific leaf area, Biogeosciences, 18, 6313–6328, https://doi.org/10.5194/bg-18-6313-2021, 2021.

Pokharel, A. K. and Obrist, D.: Fate of mercury in tree litter during decomposition, Biogeosciences, 8, 2507–2521, https://doi.org/10.5194/bg-8-2507-2011, 2011.

Rea, A. W., Keeler, G. J., and Scherbatskoy, T.: The deposition of mercury in throughfall and litterfall in the lake champlain watershed: A short-term study, Atmos. Environ., 30, 3257–3263, https://doi.org/10.1016/1352-2310(96)00087-8, 1996.

Rea, A. W., Lindberg, S. E., Scherbatskoy, T., and Keeler, G. J.: Mercury Accumulation in Foliage over Time in Two Northern Mixed-Hardwood Forests, Water Air Soil Pollut., 133, 49–67, https://doi.org/10.1023/A:1012919731598, 2002.

Richardson, J. B., Friedland, A. J., Engerbretson, T. R., Kaste, J. M., and Jackson, B. P.: Spatial and vertical distribution of mercury in upland forest soils across the northeastern United States, Environ. Pollut., 182, 127–134, https://doi.org/10.1016/j.envpol.2013.07.011, 2013.

Sanz-Cortés, F., Martinez-Calvo, J., Badenes, M. L., Bleiholder, H., Hack, H., Llacer, G., and Meier, U.: Phenological growth stages of olive trees (Olea europaea), Ann. Appl. Biol., 140, 151–157, https://doi.org/10.1111/j.1744-7348.2002.tb00167.x, 2002.

Schaefer, K., Elshorbany, Y., Jafarov, E., Schuster, P. F., Striegl, R. G., Wickland, K. P., and Sunderland, E. M.: Potential impacts of mercury released from thawing permafrost, Nat. Commun., 11, 1, https://doi.org/10.1038/s41467-020-18398-5, 2020.

Schneider, L., Allen, K., Walker, M., Morgan, C., and Haberle, S.: Using Tree Rings to Track Atmospheric Mercury Pollution in Australia: The Legacy of Mining in Tasmania, Environ. Sci. Technol., 53, 5697–5706, https://doi.org/10.1021/acs.est.8b06712, 2019.

Schwesig, D. and Krebs, O.: The role of ground vegetation in the uptake of mercury and methylmercury in a forest ecosystem, Plant and Soil, 11, 445–455, https://doi.org/10.1023/A:1024891014028, 2003.

Senesil, G. S., Baldassarre, G., Senesi, N., and Radina, B.: Trace element inputs into soils by anthropogenic activities and implications for human health, Chemosphere, 39, 343–377, https://doi.org/10.1016/S0045-6535(99)00115-0, 1999.

Sghaier, A., Perttunen, J., Sievaènen, R., Boujnah, D., Ouessar, M., Ben Ayed, R., and Naggaz, K.: Photosynthetical activity modelisation of olive trees growing under drought conditions, Sci. Rep., 9, 15536, https://doi.org/10.1038/s41598-019-52094-9, 2019.

Teixeira, D. C., Lacerda, L. D., and Silva-Filho, E. V.: Mercury sequestration by rainforests: The influence of microclimate and different successional stages, Chemosphere, 168, 1186–1193, https://doi.org/10.1016/j.chemosphere.2016.10.081, 2017.

Terral, J.-F., Alonso, N., Capdevila, R. B. i, Chatti, N., Fabre, L., Fiorentino, G., Marinval, P., Jordá, G. P., Pradat, B., Rovira, N., and Alibert, P.: Historical biogeography of olive domestication (Olea europaea L.) as revealed by geometrical morphometry applied to biological and archaeological material: Historical biogeography of olive domestication (Olea europaea L.), J. Biogeogr., 31, 63–77, https://doi.org/10.1046/j.0305-0270.2003.01019.x, 2004.

Tomiyasu, T., Matsuo, T., Miyamoto, J., Imura, R., Anazawa, K., and Sakamoto, H.: Low level mercury uptake by plants from natural environments – Mercury distribution in Solidago altissima L., Environmental Sciences: An International Journal of Environmental Physiology and Toxicology, 12, 231–238, 2005.

UNEP: Technical Background Report to the Global Mercury Assessment 2018, IVL Svenska Miljöinstitutet, Arctic Monitoring and Assessment Programme, Oslo, Norway/UN Environment

Programme, Chemicals and Health Branch, Geneva, Switzerland, viii, 426 pp., ISBN 9788279711087, 2019.

Wang, X., Lin, C.-J., Lu, Z., Zhang, H., Zhang, Y., and Feng, X.: Enhanced accumulation and storage of mercury on subtropical evergreen forest floor: Implications on mercury budget in global forest ecosystems: Hg storage on subtropical forest floor, J. Geophys. Res.-Biogeosci., 121, 2096–2109, https://doi.org/10.1002/2016JG003446, 2016.

Wofsy, S. C., Goulden, M. L., Munger, J. W., Fan, S.-M., Bakwin, P. S., Daube, B. C., Bassow, S. L., and Bazzaz, F. A.: Net Exchange of CO_2 in a Mid-Latitude Forest, Science, 260, 1314–1317, https://doi.org/10.1126/science.260.5112.1314, 1993.

Wohlgemuth, L., Rautio, P., Ahrends, B., Russ, A., Vesterdal, L., Waldner, P., Timmermann, V., Eickenscheidt, N., Fürst, A., Greve, M., Roskams, P., Thimonier, A., Nicolas, M., Kowalska, A., Ingerslev, M., Merilä, P., Benham, S., Iacoban, C., Hoch, G., Alewell, C., and Jiskra, M.: Physiological and climate controls on foliar mercury uptake by European tree species, Biogeosciences, 19, 1335–1353, https://doi.org/10.5194/bg-19-1335-2022, 2022.

Wright, L. P., Zhang, L., and Marsik, F. J.: Overview of mercury dry deposition, litterfall, and throughfall studies, Atmos. Chem. Phys., 16, 13399–13416, https://doi.org/10.5194/acp-16-13399-2016, 2016.

Yammine, P., Kfoury, A., El-Khoury, B., Nouali, H., El-Nakat, H., Ledoux, F., Courcot, D., and Aboukaïs, A.: A preliminary evaluation of the inorganic chemical composition of atmospheric tsp in the selaata region, north lebanon, Lebanese Science Journal, 11, 18, 2010.

Yanai, R. D., Yang, Y., Wild, A. D., Smith, K. T., and Driscoll, C. T.: New Approaches to Understand Mercury in Trees: Radial and Longitudinal Patterns of Mercury in Tree Rings and Genetic Control of Mercury in Maple Sap, Water Air Soil Pollut., 231, 248, https://doi.org/10.1007/s11270-020-04601-2, 2020.

Yang, Y., Yanai, R. D., Driscoll, C. T., Montesdeoca, M., and Smith, K. T.: Concentrations and content of mercury in bark, wood, and leaves in hardwoods and conifers in four forested sites in the northeastern USA, PLOS ONE, 13, e0196293, https://doi.org/10.1371/journal.pone.0196293, 2018.

Yazbeck, E. B., Rizk, G. A., Hassoun, G., El-Khoury, R., and Geagea, L.: Ecological characterization of ancient olive trees in Lebanon – Bshaaleh area and their age estimation, J. Agr. Vet. Sci., 11, 35–44, 2018.

Zhao, X. and Wang, D.: Mercury in some chemical fertilizers and the effect of calcium superphosphate on mercury uptake by corn seedlings (Zea mays L.), J. Environ. Sci., 22, 1184–1188, https://doi.org/10.1016/S1001-0742(09)60236-9, 2010

Zhou, J., Obrist, D., Dastoor, A., Jiskra, M., and Ryjkov, A.: Vegetation uptake of mercury and impacts on global cycling, Nat. Rev. Earth Environ., 2, 269–284, https://doi.org/10.1038/s43017-021-00146-y, 2021.

Zhou, J., Wang, Z., and Zhang, X.: Deposition and Fate of Mercury in Litterfall, Litter, and Soil in Coniferous and Broad-Leaved Forests, J. Geophys. Res.-Biogeosci., 123, 2590–2603, https://doi.org/10.1029/2018JG004415, 2018.